EARTH — GRAZING FIREBALLS

(The Daylight Fireball of Aug 10, 1972)

Z. *Ceplecha*, Astronomical Institute of the Czechoslovak Academy of Sciences, Ondřejov

Received 24 April 1979

Болиды с горизонтальной траекторией

(Дневной волид 10 августа 1972 г.)

В работе приведены теоретические уравнения движения метеорного тела с абляцией на почти горизонтальной траектории, которые применены к наблюденным скоростям и положениям дневного болида из 10 августа 1972 г. Установлены численные ошибки в раньше опубликованых данных по этому болиду, и исправлены после обмена несколькими письмами с авторами (таблица 1). Вычислены скорости и орбиты этого болида перед и после встречи с Землей. Тесное сближение с Землей и атмосферическое сопротивление изменило астероидальную орбиту из группы Амура в группу Аполлона. Тело может тесно сблизиться с Землей в 1997 году, когда оно будет 4 ± 8 дней от Земли. Масса тела определена в $10^5 - 10^6$ килограммов, что при данной скорости соответствует от -15 до -18 звездной величине.

Theoretical equations of motion of an ablating meteoroid in a near-horizontal trajectory are derived and applied to the observed velocities and positions of the daylight Earth-grazing fireball of Aug 10, 1972. Several numerical mistakes contained in the previously published data on this fireball have been recognized and corrected after contacting the authors (Tab. 1). The velocities and orbits of this fireball before and after encounter the Earth are computed. The close approach to the Earth and the atmospheric deceleration altered the asteroidal orbit of this meteoroid from the Amor type to the Apollo type. The body may come close to the Earth again in the year 1997 with a relative time spacing of 4 ± 8 days. The mass of the body is estimated at 10^5 to 10^6 kilograms, corresponding to a maximum absolute brightness of -15 to -18 magnitude at this velocity.

1. Introduction; Observational Data

The problems in connection with a meteoı flight along a near-horizontal trajectory differ from the common case of steep encounter, especially if the body is so big and the closest height so favorable that the rest of the body leaves the Earth to continue orbiting the Sun. Because of the existing precise observational data, now available for this case, it has proved worth-while inventing a theoretical concept of a body motion in tangential shallow trajectories with ablation of its mass. This forms one part of the paper.

A very bright fireball attracted the attention of a vast amount of casual observers and photographers in the western United States and Canada in daytime on Aug 10, 1972 (Jacchia, 1974). The trajectory of the body was unique in touching the Erath's atmosphere at slightly below 58 km. The meteoroid lost only part of its mass and continued to move in a changed orbit around the Sun. Unique observations of the fireball flight were acquired onboard a satellite by infrared radiometer tracking (Rawcliffe et al., 1974). Unfortunately the observational data of Tab. 1 in the paper of Rawcliffe et al. (1974) contain several misprints as pointed out by Carusi and Massaro (1976). The geographic positions of the three trajectory points did not correspond to the given velocities. Carusi and Massaro (1976) in their attempt to compute the orbit of the body added some more misconceptions and wrong numbers to the initial confusion.

I exchanged several letters with Charlotte D. Bartky (1978), one of the coauthors of the original paper on infrared fireball tracking. In her quick and clear responses, she sent me not only the correct data corresponding to Tab. 1 of the paper (Rawcliffe et al., 1974), but also a smooth plot of the velocity changes during the entire observed trajectory. Thus I was able to make an independent check of the relative geographic positions and heights by integrating the velocity-over-time change. A perfect match of the results finally suppressed my doubts and converted them into full confidence. The data on the fireball trajectory corrected according to Bartky (1978) are given in Tab. 1.

The main purpose of this paper is to compute the

Bull. Astron. Inst. Czechosl. 30 (1979), 349—356.

Table 1

Fireball Trajectory

Point	GMT (s)	v (km/s)	h km	φ	λ E. Gr.
1 Initial	73 708·9	15·03	75·98	39·289°	247·425°
2 Perigee	73 747·5	14·60	57·85	44·386°	247·007°
3 Final	73 810·1	14·21	101·55	52·331°	246·242°

v velocity according to a fixed Earth surface (φ, λ system)
h height with respect to the surface of the geoid of 1971
φ geographic latitude
λ geographic longitude East of Greenwich

orbits of the body before and after the encounter with the Earth. The detected trajectory and the changes of velocity due to the atmospheric drag have to be studied first. They will yield data necessary for computation of accurate orbits.

2. The Curved Fireball Trajectory

Without the atmosphere, the observed trajectory would be a section of a hyperbola in the vicinity of its vertex, the perigee. The actual trajectory is somewhat more curved due to the loss of velocity by air drag. In any case the curved trajectory can be substituted by osculating circles with sufficient accuracy. I will use two osculating circles, one before the perigee and the other after the perigee. In both cases I define these circles as being horizontal at the perigee and passing the point 1 (Initial) or 3 (Final) of Tab. 1, respectively. The situation is schematically given in Fig. 1.

I will compute the directions, heights and velocities at the two middle points between 1 and 2 or 2 and 3. The radius, R_c, of the first osculating circle can be computed from intersection C of the vertical line through point 2 with the plane passing through the middle point M between 1 and 2 and being perpendicular to the vector from point 1 to point 2. If we denote $\psi \equiv \sphericalangle$ point 1, C, point 2 and $d \equiv$ the distance from point 1 to point 2, we have

$$R_c = \frac{d}{2 \sin (\psi/2)} \,. \tag{1}$$

The radius of the second osculating circle can be computed from (1), if point 1 in the preceding consideration is substituted by point 3.

The numerical results are in Tab. 2. The geocentric latitude φ' at the height h of the corresponding point was computed from

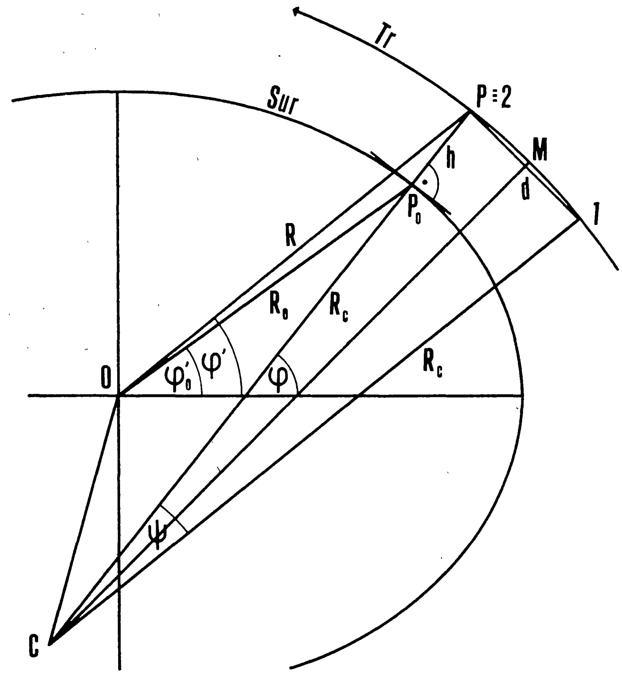

Fig. 1. A schematic plot of the osculation circle of the Aug 10 fireball trajectory (*Tr*) defined as being horizontal at point 2 and passing through point 1. "Sur" is the eliptical Earth's surface and the other notations are referred to in the text. Note that the trajectory of the daylight fireball of Aug. 10, 1972 was almost in the meridian plane.

$$\varphi' = \varphi'_0 + \frac{h}{R_0 + h} (\varphi - \varphi'_0) \,, \tag{2}$$

where the geocentric latitude φ'_0 on the surface is (Transactions of the IAU, 1977)

$$\varphi'_0 = \varphi - 0{\cdot}1924240867° \sin 2\varphi + 0{\cdot}000323122° \sin 4\varphi - 0{\cdot}0000007235° \sin 6\varphi \tag{3}$$

and the radius vector R_0 on the surface is (in kilometers):

$$R_0^2 = 40680669{\cdot}86 \, \frac{1 - 0{\cdot}0133439554 \sin^2 \varphi}{1 - 0{\cdot}006694385096 \sin^2 \varphi} \,. \tag{4}$$

The radius vector to the corresponding point at the height h is then

$$R = R_0 + h \,, \tag{5}$$

where the difference of directions of R_0 and h can be neglected without any impact on the precision of the results. The geocentric rectangular coordinates are then given by

(6)
$$X = R \cos \varphi' \cos \lambda$$
$$Y = R \cos \varphi' \sin \lambda$$
$$Z = R \sin \varphi' ,$$

where λ is the longitude.

The vertical vector at point 2 of unit length is given by geographic latitudes and is evaluated for our special case

(7)
$$x_2 = \cos \varphi_2 \cos \lambda_2 = -0{\cdot}27915314$$
$$y_2 = \cos \varphi_2 \sin \lambda_2 = -0{\cdot}65786703$$
$$z_2 = \sin \varphi_2 = 0{\cdot}69948874 .$$

The plane perpendicular to the vector from point 1 to point 2 contains unit vectors x, y, z given by

(8)
$$0{\cdot}21044166x + 0{\cdot}65889950y + 0{\cdot}72219510z = 0 ,$$

where the coefficients are the coordinates of the vector from point 1 to point 2 divided by its length $d = 573{\cdot}247$ km. The scalar product of these coefficients with the vertical vector at point 2 is equal to

Table 2

Point	1 Initial	2 Perigee	3 Final
φ'_0	39·10051°	44·19363°	52·14468°
φ'	39·10273°	44·19536°	52·14761°
R_0 [km]	6369·608	6367·722	6364·783
R [km]	6445·588	6425·572	6466·333
X [km]	−1920·185	−1799·550	−1598·578
Y [km]	−4618·627	−4240·915	−3631·670
Z [km]	4065·315	4479·311	5105·779

Point on the osculating circle	Middle between 1 and 2	Middle between 2 and 3
d [km]	573·247	896·678
$\psi/2$	0·7422095°	1·1947748°
R_c [km]	22126·86	21501·79
t GMT	$20^h28^m48{\cdot}1^s$	$20^h29^m38{\cdot}6^s$
φ'	41·64527°	48·18471°
φ'_0	41·64342°	48·18267°
φ	41·83460°	48·37384°
λ	247·22459°	246·65301
R [km]	6431·06	6435·04
h [km]	62·39	68·80
v [km/s]	14·869	14·264
	± ·005	± ·005
v_∞ [km/s]	15·083	14·208
	± ·019	± ·005
α_R apparent	158·899°	158·566°
	± ·010	± ·010
δ_R apparent	−46·236°	−44·319°
	± ·010	± 0·010

$\sin (\psi/2)$ and, thus R_c can be computed from relation (1).

The plane perpendicular to the vector from point 2 to point 3 contains unit vectors x, y, z given by

(9)
$$0{\cdot}22412952x + 0{\cdot}67944683y + 0{\cdot}69865440z = 0 ,$$

where the coefficients are the coordinates of the vector from point 2 to point 3 divided by its length $d = 896{\cdot}678$ km. The resulting angles $\psi/2$ and the radii R_c are given in Tab. 2.

The data at the middle points between 1 and 2 or 2 and 3 are also given in Tab. 2. The smooth plot of the velocity against time (Bartky, 1978) was converted into the velocity against the height by means of computing the total length of the trajectory from the perigee point as it will be described in chapter 3. Thus the time, the height and the velocity were determined at the middle point of the total length measured along the osculating circle (from the perigee to point 1, and from the perigee to point 3). The geocentric and geographic coordinates of these middle points were also computed. It is interesting to compare the heights of the middle points on the osculating circles with the heights at the middle points on the straight line connecting points 1 and 2 or 2 and 3. The middle points on the osculating circles are 1·86 km and 5·84 km higher than the corresponding points on the straight lines connecting point 1 and 2 or 2 and 3, respectively.

The directions of the vectors from point 2 to point 1 and from point 3 to point 2 were converted into right ascensions α_R and declinations δ_R of the apparent radiant of the body motion relatively to the fixed Earth's surface at the middle points. These two vectors are exactly parallel to the two instantaneous directions of the body at the two middle points on the osculating circle.

3. The Velocities

As already mentioned, I have more velocity data available (Bartky, 1978) than that in the original paper (Rawcliffe et al., 1974). The smooth plot of the velocity against time can be used

a) as a good check of the positional data in Tab. 1.

b) to study the atmospheric deceleration and to compute the no-atmosphere velocities.

For this purpose I used not only osculation circles to substitute the fireball trajectory as given in chapter 2, but also osculation circles to substitute the ellipse of the Earth's surface section (Fig. 2). The numerical procedure followed that described for the trajectory

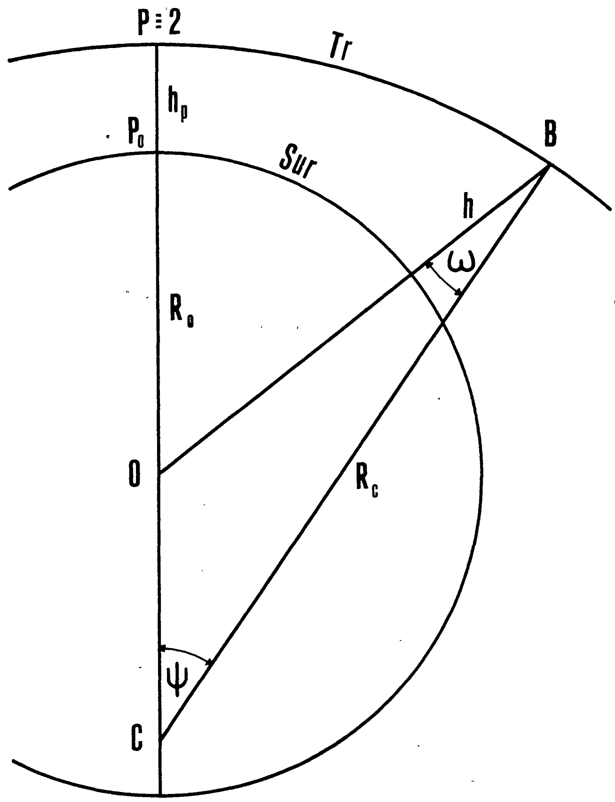

Fig. 2. A schematic plot of the osculation circles of the Earth's surface (*Sur*) and of the trajectory (*Tr*) as used for integrating the velocities and computing the heights in Tab. 3. The notations are referred to in the text.

osculation, and the osculation radii of the Earth's surface then resulted: $R_0 = 6364{\cdot}747$ km between point 1 and 2; $R_0 = 6369{\cdot}677$ km between point 2 and 3. If we denote $\psi \equiv \sphericalangle PCB$, $R_c \equiv CP = CB$ the osculating radius of the trajectory, l the total length of the curved trajectory from P to B, and h_p the height at the perigee, and if the velocity is given as a function of time $v = v(t)$, we can compute l by integrating

$$\mathrm{d}l = v \, . \, \mathrm{d}t \tag{10}$$

and determine ψ from

$$\psi = \frac{l}{R_c} \tag{11}$$

and the height from

$$h = \sqrt{[4[R_c^2 - R_c(R_0 + h_p)] \, . \, \sin^2 \tfrac{1}{2}\psi + (R_0 + h_p)^2]} - R_0 \, . \tag{12}$$

The numerical values of the velocities were taken from the smooth plot for each integer time second and the integration of (10) was performed by the Runge-Kutta method starting from the perigee with $l = 0$ and going back in time for the trajectory part before the perigee and forward in time for the part after the peıigee. Thus h and l were obtained for each integer time second. Some of these values are given in Tab. 3 for 10 different times. The heights resulting from equation (12) and the heights corrected to positional data of Tab. 1 are given for comparison.

Table 3

Observed velocities and computed heights at selected points (with respect to the fixed Earth's surface)

GMT [s]	v [km/s]	Eq. (12) h [km]	Eq. (12) corrected to Tab. 1 h [km]
73 708·9	15·030	75·98	75·98
73 720·0	14·954	66·99	66·99
73 730·0	14·846	61·52	61·52
73 740·0	14·711	58·52	58·52
73 747·5	14·602	57·85	57·85
73 750·0	14·565	57·92	57·92
73 760·0	14·427	59·64	59·64
73 770·0	14·314	63·61	63·62
73 780·0	14·258	69·78	69·79
73 790·0	14·231	78·13	78·16
73 800·0	14·216	88·66	88·70
73 810·1	14·210	101·49	101·55

The total computed length of the trajectory before the perigee (from the perigee at 73 747·5 s to point 1 at 73 708·9 s) resulted from Eqs (10) and (11) as 573·22 km, while the same value computed quite independently from the positions given in Tab. 1 turned out to be 573·26 km. This is perfect agreement and, if the positions in Tab. 1 are assumed as fixed, the systematic error in the velocities taken from the smooth plot before the perigee is only $-0{\cdot}001$ km/s. The total computed length of the trajectory after the perigee (from the perigee at 73 747·5 s to point 3 at 73 810·1 s) resulted from Eqs (10) and (11) as 896·10 km, while the same value, but independently determined from positions in Tab. 1, was computed as 896·74 km. This is still very good agreement indicating a systematic error of $-0{\cdot}010$ km/s in velocities taken from the plot as compared with the fixed ("no-erroı") positions of Tab. 1. The heights computed from equation (12) are also in good agreement with those directly given in Tab. 1. If we consider the cumulative nature of errors in performing the integration and the graphical character of the input velocity data, we have to be very satisfied by the perfect agreement of the positional and velocity data.

4. Theory of Ablating Body in a Near-horizontal Trajectory; No-atmosphere Velocities

We need a theoretical approach to derive the no-atmosphere velocities from the observed values. Since the extrapolation of the observed velocity to the no-atmosphere value is quite a small correction with such a big body, the inaccuracy originating from simple assumptions of the theory should be insignificant.

The equations of a body moving through the atmosphere and ablating at the same time can be written:

$$\frac{dv}{dt} = -\Gamma A \varrho_m^{-2/3} m^{-1/3} \varrho v^2 \tag{13}$$

$$\frac{dm}{dt} = -\frac{\Lambda A \varrho_m^{-2/3}}{2\zeta} m^{2/3} \varrho v^3 \tag{14}$$

$$\frac{dh}{dt} = v \sin\omega\,, \tag{15}$$

where v, m, h, ϱ are the instantaneous values of the velocity, the mass, the height and the air density at time instant t, respectively, where ω is the inclination of the direction of the body motion to the instantaneous horizon, ϱ_m is the density of the body, A is a geometrical shape factor ($A = s m^{-2/3} \varrho_m^{2/3}$, if s is the head cross-section), Γ the drag coefficient, Λ the heat transfer coefficient, ζ the energy necessary for ablation of unit mass of the body. These "classical" equations are also known as the "single body theory" in meteor physics, because they do not express an eventual fragmentation of the body. We will assume all the parameters Γ, Λ, A, ζ and ϱ_m to be constant. Usually, in solving Eqs (13) to (15) for a meteor body, the inclination, ω, of its straight-line trajectory to the instantaneous horizon is also taken as a constant value neglecting the curvature of the Earth's surface. But in our case, ω decreases to zero and starts to increase again and the length of the curved trajectory is so large that the curvature of the Earth's surface, as well as of the trajectory, must be considered. Thus, we will assume ω as a function of time and solve the Eqs (13) to (15) for a curved near-horizontal trajectory.

Dividing Eqs (14) by (15), separating the variables m and v and integrating, we have

$$m = m_\infty \exp\left[\tfrac{1}{2}\sigma(v^2 - v_\infty^2)\right], \tag{16}$$

where the ablation coefficient, σ, is given by

$$\sigma = \frac{\Lambda}{2\zeta\Gamma} \tag{17}$$

and m_∞ and v_∞ are the mass and velocity outside the atmosphere ($h \to \infty$). Substituting (16) into (13), we have

$$\frac{dv}{dt} = -\Gamma A \varrho_m^{-2/3} m_\infty^{-1/3} \exp\left[\tfrac{1}{6}\sigma(v_\infty^2 - v^2)\right] \varrho v^2\,. \tag{18}$$

If we could change the independent variable t in Eq. (18) into the independent variable h, we would be able to integrate the equation assuming ϱ to be a known function of height. This can be done by expressing the angle ω as a function of height.

In Fig. 2, P is the perigee of the meteoroid body (point 2), B the instantaneous position of the body, O the center of the osculating circle of the geoid section (horizontal at P_0), C the center of the osculating circle of the trajectory (horizontal at P). If we denote R_c the radius of osculating circle of the trajectory, R_0 the radius of osculating circle of the geoid, h_p the height at perigee, h the height at B, then $OB = R_0 + h$, $OC = R_c - R_0 - h_p$, $BC = R_c$, and from the triangle OCB for the angle $\omega = \sphericalangle\, OBC$ we find

$$\sin\frac{\omega}{2} = \sqrt{\left[\frac{(R_c - R_0 - \frac{1}{2}h - \frac{1}{2}h_p)(h - h_p)}{2R_c(R_0 + h)}\right]} \tag{19}$$

R_c is at least several times greater than R_0 at hyperbolic geocentric velocities and $\frac{1}{2}h$ and $\frac{1}{2}h_p$ are quite negligible relatively to the difference $R_c - R_0$; also h is a second order term in $R_0 + h$. In case of the near-horizontal trajectory, the angle ω is small enough to assume $\sin\frac{1}{2}\omega \doteq \frac{1}{2}\sin\omega$. Thus, we can write (19) with sufficient first order accuracy as

$$\sin\omega \doteq \sqrt{\left[\frac{2(R_c - R_0)}{R_c R_p}\right]} \cdot \sqrt{(h - h_p)}\,, \tag{20}$$

where R_p is, in the first approximation, a constant, which should slightly exceed the maximum value of all $R_0 + h$ considered. Equation (20) expresses the direction of flight according to the instantaneous horizon as a function of the instantaneous height and can be directly substituted into Eq. (15):

$$\frac{dh}{dt} = \pm v \sqrt{\left[\frac{2(R_c - R_0)}{R_c R_p}\right]} \cdot \sqrt{(h - h_p)}\,, \tag{21}$$

where the minus sign holds for the trajectory before the perigee and the plus sign holds for the trajectory after the perigee.

Now substituting (21) into (18), separating the variables and integrating from h to ∞ with

$$\varrho = \varrho_p \exp\left[b(h_p - h)\right], \tag{22}$$

where ϱ_p is the air density at the perigee and b is the air density gradient (assumed to be constant), we have before the perigee

(23)
$$\overline{\mathrm{Ei}}\left(\frac{\sigma v_{\infty B}^2}{6}\right) - \overline{\mathrm{Ei}}\left(\frac{\sigma v^2}{6}\right) = \varkappa_B \operatorname{erfc} \sqrt{[b(h - h_p)]}$$

and after the perigee

(24)
$$\overline{\mathrm{Ei}}\left(\frac{\sigma v^2}{6}\right) - \overline{\mathrm{Ei}}\left(\frac{\sigma v_{\infty E}^2}{6}\right) = \varkappa_E \operatorname{erfc} \sqrt{[b(h - h_p]} ,$$

where the constants are given by

(25)
$$\varkappa_B = 2\Gamma A \varrho_m^{-2/3} m_{\infty B}^{-1/3} \varrho_p \sqrt{\left[\frac{\pi R_p R_{CB}}{2b(R_{CB} - R_0)}\right]} . \exp\left(\frac{\sigma}{6} v_{\infty B}^2\right)$$

(26)
$$\varkappa_E = 2\Gamma A \varrho_m^{-2/3} m_{\infty E}^{-1/3} \varrho_p \sqrt{\left[\frac{\pi R_p R_{CE}}{2b(R_{CE} - R_0)}\right]} . \exp\left(\frac{\sigma}{6} v_{\infty E}^2\right).$$

Here the subscripts B, E are used for the values before and after the perigee, respectively. $\overline{\mathrm{Ei}}(x) = \int_0^{e^x} (e^u/u) \, du$ is the logarithmic integral and

$$\operatorname{erfc}(x) = \frac{2}{\sqrt{\pi}} \int_x^\infty e^{-u^2} \, du$$

is the error function.

There are 4 unknown parameters to be determined in Eqs (23) or (24): σ, $v_{\infty B}$, $\varkappa_B$, b and σ, $v_{\infty E}$, $\varkappa_E$, b, respectively. We are mostly interested in the velocities $v_{\infty B}$ and $v_{\infty E}$, which are the no-atmosphere values to be applied to computing the orbits before and after the perigee, if the atmospheric drag is taken into consideration.

The solution of the unknown parameters in Eqs (23) and (24) can be done by linearizing them according to the unknown parameters for the purpose of the least-squares fit to the observed velocities. All partial derivatives of (23) or (24) necessary to compute the total differentials can be expressed analytically. Thus the least squares can be used for computing differentials of any initial set of values σ, v_∞, $\varkappa$, b, these values corrected and used again as initial values. I used the observed velocities for each integer time second and compared them with values computed from (23) or (24), respectively. The following solutions were obtained:

before the perigee: $v_{\infty B} = 15{\cdot}074 \pm 0{\cdot}018$ km s^{-1}, $\sigma = 0{\cdot}0485$ km^{-2} s^2, $\varkappa_B = 0{\cdot}393$, $b = 0{\cdot}072 \pm 0{\cdot}016$ km^{-1} and after the perigee: $v_{\infty E} = 14{\cdot}212 \pm 0{\cdot}001$ km s^{-1}, $\sigma = 0{\cdot}0187$ km^{-2} s^2, $\varkappa_E = 0{\cdot}104$, $b = 0{\cdot}105 \pm$ $\pm$ $0{\cdot}003$ km^{-1}.

The standard deviations of σ and $\varkappa$ came out the same order as the values themselves. The average standard deviation of any comparison of observed velocity with Eq. (23) and (24) turned out to be $\pm 0{\cdot}007$ and $\pm 0{\cdot}003$ km s^{-1}, respectively. Small systematic deviations of the computed velocities from the observed values are evident from the residua. They are inside of $+0{\cdot}019$ and $-0{\cdot}004$ km s^{-1} for the solution before the perigee, and inside of $+0{\cdot}004$ and $-0{\cdot}004$ km s^{-1} for the solution after the perigee. Evidently, the Eqs (23) or (24) are only interpolation formulae, when applied to the observations of the velocities of this fireball and the only resulting values we can dwell upon are the no-atmosphere velocities $v_{\infty B}$ and $v_{\infty E}$. It is not possible to check the theoretical considerations by means of these observations; observations at least one order of accuracy higher would be necessary to determine anything definitive about resulting σ and $\varkappa$. The solutions with a fixed b (that of the real atmosphere) and only three free parameters yielded even worse fits than the 4 free-parameter solutions.

The resulting no-atmosphere values corrected for the mentioned systematic deviations are

$$v_{\infty B} = 15{\cdot}083 \pm 0{\cdot}019 \text{ km/s}$$
$$v_{\infty E} = 14{\cdot}208 \pm 0{\cdot}005 \text{ km/s}$$

5. The Orbits

The classical approach of computing meteor orbits was applied to the dynamic and positional data of this fireball. These computations may be described as "double two-body" solutions. The observed velocity vector at the middle point (v, radiant α_R, δ_R) was corrected for the Earth's rotation and than changed into the no-atmosphere value without changing its direction. This velocity vector was corrected for the Earth's gravity assuming a hyperbolic trajectory around the Earth's center. The asymptotic values of this hyperbola (v_G, radiant α_G, δ_G) are the geocentric values. If the Earth's velocity vector is subtracted from this geocentric velocity vector of the meteoroid, the resulting heliocentric velocity vector of the body and the instantaneous position of the Earth in its orbit determine the orbit of the fireball body around the Sun. The numerical results are given in Tab. 4.

Table 4

The Orbits (1950·0)

	Before Encounter	After Encounter
v_G km/s	10·15 $\pm$ ·03	8·804 $\pm$ ·008
α_G	159·00° $\pm$ ·02	155·538° $\pm$ ·007
δ_G	$-$67·48 $\pm$ ·08	$-$19·05° $\pm$ ·03
v_H km/s	34·88 $\pm$ ·02	33·878 $\pm$ ·006
ε_G	114·696° $\pm$ ·016	113·445° $\pm$ ·009
ε_H	164·67° $\pm$ ·03	166·206 $\pm$ ·010
a A.U.	1·661 $\pm$ ·004	1·4715 $\pm$ ·0009
e	0·3904 $\pm$ ·0016	0·3633 $\pm$ ·0004
q A.U.	1·0127 $\pm$ ·0000	0·9369 $\pm$ ·0000
Q A.U.	2·310 $\pm$ ·009	2·0061 $\pm$ ·0019
ω	355·57° $\pm$ ·08	315·76° $\pm$ ·02
Ω	317·956°	317·949°
i	15·22° $\pm$ ·03	6·928° $\pm$ ·012
ΔT days	3·90 $\pm$ ·07	36·80 $\pm$ ·02

v_G geocentric velocity
α_G, δ_G right ascension and declination of the geocentric radiant
v_H heliocentric velocity
ε_G, ε_H elongation of the geocentric and heliocentric radiant from the Earth's apex
Q aphelion distance
ω argument of perihelion
ΔT time elapsed from the perihelion passage to the encounter

The authors (Rawcliffe et al., 1974) did not disclose the standard deviations of their observations. The standard deviations in Table 4 were computed assuming a value of $\pm 0{\cdot}01°$ in the right ascension and declination of the radiant as it was estimated from the comparison of the positional and velocity data. The standard deviations of the velocities were computed from the least-squares solutions in chapter 4.

The orbit before encounter with the Earth is in perfect agreement with the previous computations of McCrosky (1974). The close approach to the Earth and the atmospheric deceleration changed the asteroidal orbit of the meteoroid from the Amor type to the Apollo type. The body may come close to the Earth again after 14 revolutions with a relative time spacing of 4 $\pm$ 8 days in the year 1997.

6. The Mass

The mass of the body remains very uncertain. If we substitute the least-squares solutions of v_∞, σ, $\varkappa$, b into equations (25) or (26), and if we assume the body density $\varrho_m = 3{\cdot}7$ g cm^{-3}, and $\Gamma A = 1{\cdot}20$, we obtain $\log m_{\infty E} = 4{\cdot}3 \pm 2{\cdot}1$ (in kg) while $\log m_{\infty B}$ cannot be realisticly determined. The dynamic mass computed from the deceleration at the perigee with the same ϱ_m and ΓA came out as $\log m = 4{\cdot}4 \pm 1{\cdot}8$ (in kg). If the body density is assumed similar to that of carbonaceous chondrites, the computed mass is almost 10^5 kg. If the luminous efficiency (Ceplecha and McCrosky, 1976) is applied to the above computed masses, the maximum brightness can be schematically computed according to McCrosky (1968). This resulted in -14 ± 5 stellar magnitude for the density of ordinary chondrites and in -15 ± 5 stellar magnitude for the density of carbonaceous chondrites. Thus the observed decelerations correspond, within the standard deviations, to the visually estimated brightness.

Jacchia (1974) evaluated the mass range from thousands to a million metric tons using the estimates of the fireball brightness. But his computations must contain a numerical mistake of about two orders of magnitude: either he took an extremely low luminous efficiency, inconsistent with the present knowledge based on experiments, or he made a mistake by 5 stellar magnitudes. If the luminous efficiency had been taken from the paper of Ceplecha and McCrosky (1976, Tab 1 on page 6259), and the density $\varrho_m = 3{\cdot}7$ g cm^{-3} assumed, the photometric mass would then have resulted in 70 metric tons for -15 maximum stellar magnitude of the object at a distance of 100 km, or in 3000 metric tons for -19 maximum stellar magnitude at a distance of 100 km.

The authors of the observations (Rawcliffe et al., 1974) estimated 1000 tons from the recorded thermal radiation, but assuming that the whole change of kinetic energy was transformed into thermal radiation.

Thus 10^5 to 10^6 kg seems to be the most probable range of the actual mass of the body. This mass corresponds to a maximum brightness of between -15 and -18 stellar magnitude, which seems quite reasonable. In any case the discrepancy in computing the mass of the body using dynamic and photometric data is the well-known paradox of meteor physics and it will be avoided by a better understanding of all processes involved in big bodies encountering our atmosphere.

Acknowledgment

I am very much indebted to Mrs. Charlotte D. Bartky from the Aerojet Electro Systems in Azusa, California, for sending me the corrected data of Tab. 1 and especially for putting at my disposal the unpublished smooth plot of the measured velocities against time. My special thanks are due to Dr. Andrea Carusi from the "Laboratorio Astrofisica Spaziale" in Rome for discussions on the problems of the fireball orbit computations. I am very greatful to Dr. Ian Halliday from the Herzberg Institute of Astrophysics in Ottawa, who gave me the opportunity to compare the results of his and my computer programs in evaluating the photographic orbit of the Innisfree meteorite fall, which helped to improve appreciably the work and precision of my orbital program.

REFERENCES

Bartky, C. D.: 1978, The Smooth Velocity Plot (private commun.).

Carusi, A.; Massaro, E.: 1976, Astrophys. Letters **17**, 113.

Ceplecha, Z.; McCrosky, R. E.: 1976, J. Geophys. Res. **81**, 6257

Jacchia, L. G.: 1974, Sky and Telescope **48**, 4.

McCrosky, R. E.: 1968, Smithson. Astrophys. Spec. Rep. No. 280.

Rawcliffe, R. D.; Bartky, C. D.; Li, F.; Gordon, E.; Carta, D.: 1974, Nature **247**, 449.

Transactions of the International Astronomical Union XVI B, 1977, (Ed. E. A. Müller and A. Jappel; D. Reidel Publ. Co., Dordrecht), p. 58.

Z. Ceplecha
Astronomical Institute
Czechoslovak Academy of Sciences
251 65 Ondřejov
Czechoslovakia